Check for updates

# Breakup without borders: how continents speed up and slow down during rifting

Martina M. Ulvrova[1], Sascha Brune[2,3], and Simon Williams[4]

Corresponding author: M. Ulvrova, Department of Earth Sciences, Institute of Geophysics, ETH Zürich, Sonneggstrasse 5, Zürich, 8092, Switzerland. (martina.ulvrova@erdw.ethz.ch)

[1]Institute of Geophysics, ETH Zürich, Zürich, Switzerland.

[2]GFZ German Research Centre for Geosciences, Potsdam, Germany.

[3]Institute of Earth and Environmental Science, University of Potsdam, Potsdam, Germany

[4]EarthByte Group, School of Geosciences, University of Sydney, Sydney, New South Wales, Australia

Accepted Article

This article has been accepted for publication and undergone full peer review but has not been through the copyediting, typesetting, pagination and proofreading process, which may lead to differences between this version and the Version of Record. Please cite this article as doi: 10.1029/2018GL080387

©2018 American Geophysical Union. All Rights Reserved.

Relative plate motions during continental rifting result from the interplay of local with far-field forces. Here, we study the dynamics of rifting and breakup using large-scale numerical simulations of mantle convection with self-consistent evolution of plate boundaries. We show that continental separation follows a characteristic evolution with four distinctive phases: (1) An initial slow rifting phase with low divergence velocities and maximum tensional stresses, (2) a syn-rift speed-up phase featuring an abrupt increase of extension rate with a simultaneous drop of tensional stress, (3) the breakup phase with inception of fast sea-floor spreading and (4) a deceleration phase occurring in most but not all models where extensional velocities decrease. We find that the speed-up during rifting is compensated by subduction acceleration or subduction initiation even in distant localities. Our study illustrates new links between local rift dynamics, plate motions and subduction kinematics during times of continental separation.

**Keypoints:**

- We investigate rift dynamics without imposed lateral boundaries using 2D spherical annulus numerical models.
- Continental rupture exhibits a multiphase evolution: 1) slow rifting 2) sudden acceleration prior to breakup 3) fast drifting 4) drift slow-down
- Abrupt plate speed-up during rifting induces subduction initiation or generates enhanced convergence at existing plate boundaries

©2018 American Geophysical Union. All Rights Reserved.

Accepted Article

## 1. Introduction

Rifting of continents is an integral component of the Wilson cycle and a key ingredient in Earth's plate tectonic history, being the geodynamic process that forms new continental margins. Rift velocity is thought to be one of the key parameters controlling fault evolution and rift symmetry [Huismans and Beaumont, 2003; Brune et al., 2014; Tetreault and Buiter, 2018], while the rate of extension also governs melt production and affects the volcanic or magma-poor nature of rifted margins [Pérez-Gussinyé et al., 2006; Davis and Lavier, 2017; Lundin et al., 2018]. Nevertheless, the geodynamic factors that control the evolution of rift velocity and strain localization from inception of rifting to breakup of continents and beyond are not understood in detail [Ziegler and Cloetingh, 2004; Buck, 2015; Brune, 2016].

Rift velocities for specific rifted margins can be estimated by combining full-fit plate reconstructions with available geological indicators such as syn-rift sedimentation, rift-related volcanism, seismic tectono-stratigraphy and dated rocks from the continent-ocean transition [Buck, 2015]. Many margins appearto involve a slow initial rift phase followed by a characteristic increase of the rift velocity and finally a fast rift phase prior to continental separation [e.g. McQuarrie and Wernicke, 2005; Kneller et al., 2012; Heine et al., 2013]. Concurrently, a characteristic rift velocity evolution can be inferred from analytical or numerical models of lithospheric extension, which reproduces the observed slow/fast velocity evolution and shows that the loss of rift strength is responsible for the abrupt rift acceleration [Brune et al., 2016].

Accepted Article

©2018 American Geophysical Union. All Rights Reserved.

Previous numerical rift models belongto one of two categories. Models with velocity boundary conditions usually impose constant velocities at the lateral model sides, which allows to study the effect of extension rate on rift processes [e.g. Ammann et al., 2017; Brune et al., 2017; Armitage et al., 2018]. More complex setups involve temporarily varying velocities to match observations [e.g. Koptev et al., 2015; Naliboff and Buiter, 2015; Salerno et al., 2016] or spatially varying velocities mimicking basin opening around an Euler pole [Mondy et al., 2017]. All of these models however, have the disadvantage that rift velocities have to be known a priori. A second category of models apply a constant extensional force in order to investigate how rift velocities evolve through time [Takeshita and Yamaji, 1990; Brune et al., 2012, 2013]. These models nonetheless suffer from the limitation that the force applied at the model boundaries is uniform through time. Another problem of rift models with force boundary conditions is that the necking instability, i.e. the rift localization during thinning of the lithosphere, leads to exponentially growing rift velocities [Takeshita and Yamaji, 1990], such that the bulk extension rates eventually reach unrealistically high values unless a switch to velocity boundary conditions at a limiting velocity is implemented [Heine and Brune, 2014].

The problem of reproducing rift velocity evolution in models with imposed lateral boundary conditions is linked to the simple fact that there are no lateral boundaries in nature. Instead, the plate-tectonic driving forces slab pull, basal drag and ridge push [Forsyth and Uyeda, 1975], which ultimately derive from buoyancy variations in Earth's interior, interact with local rift forces such as rift strength, topography-induced

Accepted Article

©2018 American Geophysical Union. All Rights Reserved.

tension and thermal buoyancy [Brune, 2018] in a self-consistent manner that can neither be fully described through velocity nor force boundary conditions.

In this study, we investigate the pre-, syn-, and post-rift dynamics of continental extension using 2D spherical annulus models of mantle convection with continents. Similar models have been previously used to study supercontinent cyclicity statistically [Rolf et al., 2014] but here, we focus on the dynamics of rifting. In contrast to previous regional rift models, our simulations avoid the necessity to impose lateral boundary conditions so that rifting develops self-consistently as a response to the overall dynamics of the system. After introducing the model setup, we describe 10 different model scenarios and compare their velocity evolutions to plate tectonic reconstructions of key natural examples. In doing so we propose 4 characteristic phases to describe extensional evolution and suggest potential causes for each phase.

## 2. Model setup

To capture the dynamics of the Earth's interior and its surface expression, we solve for the equations of conservation of mass, momentum and energy and for the advection of different material compositions . Temperature, pressure, velocity flow and composition solutions are found in dimensionless space and have to be scaled in order to be compared to Earth dynamics (for non-dimensional equations and governing parameters, description of the initial conditions and scaling procedure see supplement [Turcotte and Schubert, 2002; Coltice et al., 2012; Müller et al., 2016]).

In our model, the mantle is heated from the core and from within. The internal heating rate is set to $H = 20$ that corresponds to $2.77 \times 10^{-11}\,\mathrm{W\,kg^{-1}}$. This value of $H$ results

©2018 American Geophysical Union. All Rights Reserved.

Accepted Article

in a system that is controlled by the dynamics of the top boundary layer while thecore contributes about 20% to the total surface heat budget, which falls into the estimated interval for the Earth of 10%-40% [Jaupart et al., 2015]. Both, the top and the bottom boundaries are kept isothermal and free slip so that we neglect vertical deformation of the surface and development of topography. Compared to regional rift models, our set-up does not require any lateral boundary conditions. This advantage is balanced by lower resolution compared to lithospheric-scale models.

Viscosity $\eta$ is strongly temperature dependent and follows the Arrhenius law

$$\eta(T,p) = \eta_A \exp\left(\frac{E_a + p\,V_a}{RT}\right), \tag{1}$$

with $V_a = 6.34 \cdot 10^{-7}\,\mathrm{m^3\,mol^{-1}}$ the activation volume and $E_a = 170\,\mathrm{kJ\,mol^{-1}}$ the activation energy. $R$ is the gas constant, $T$ the absolute dimensional temperature and $p$ the pressure. $\eta_A$ is set such that $\eta$ matches the reference viscosity $\eta_0$ at temperature 1600 K and at zero pressure. We apply a viscosity cut-off at $10^4\,\eta_0$ to limit the viscosity variations to 6 orders of magnitude over $\Delta T$, the temperature drop over the mantle.

In order to localise strain and obtain a plate-like surface, we adopt pseudo-plastic yielding [Moresi and Solomatov, 1998; Tackley, 2000a, b]. Rocks are softened and viscosity decreases with increasing strain rate $\dot{\epsilon}$ beyond a certain stress threshold, the yield stress $\sigma_\mathrm{Y}$ according to: $\eta_\mathrm{Y} = \sigma_\mathrm{Y}/(2\dot{\epsilon})$. $\sigma_\mathrm{Y}$ is parameterized via a surface yield stress and a yield gradient that describes a linearly increasing yield stress with depth. Yielding parameters are listed in supplementary Table 1 together with physical parameters of the model given in supplementary Table 2.

©2018 American Geophysical Union. All Rights Reserved.

Accepted Article

We also prescribe weak oceanic crust that decouples to a certain degree the sinking slab from the overriding plate causing subduction asymmetry [Tagawa et al., 2007; Gerya et al., 2008; Crameri et al., 2012]. The crust is neutrally buoyant, and it follows the same viscosity law as ambient mantle while being 10 times less viscous and more easily deformable. The thickness of the crust is 20 km so that it can be resolved numerically (having at least two 10 km thick grid cells within the crustal material). It is formed at the ridges,dives back to the mantle at the trenches, and after reaching 290 km depthis converted to regular mantle material. Using such rheology results in self-consistent formation of strong plate interiors moving with a constant velocity delimited by narrow plate boundaries with reduced viscosity. Importantly, such rheology is sufficiently realistic to investigate global surface tectonics [Coltice et al., 2017].

Continental rafts are modeled using tracers [Tackley and King, 2003; Rolf and Tackley, 2011; Rolf et al., 2017]. We consider two continents of identical shape with interiors that are 300 km thick and 3600 km wide surrounded by 140 km thick belts following the thickness of Archean cratons and Proterozoic belts. The width of the belts is 1200 km. At each time step, continents cover in total 30% of the model surface. To ensure the stability of the continents, two conditions must be fulfilled: positive buoyancy and limited deformation within continents [e.g. Doin et al., 1997; Lenardic and Moresi, 1999]. We choose a density contrast between continental material and ambient mantle of $-100\,\mathrm{kg\,m^{-3}}$ that gives a buoyancy ratio (ratio between the density contrast and the thermal density variation) of -0.4. Continents are 100 times more viscous than the ambient mantle and either feature a high yield stress or are entirely exempted from plastic deformation (cf.

©2018 American Geophysical Union. All Rights Reserved.

Accepted Article

supplementary Table 1). Due to the high rigidity, continental erosion by mantle flow is negligible and the rafts are stable over billions of years.

We run the simulations using the StagYY code [Tackley, 2008] in spherical annulus geometry [Hernlund and Tackley, 2008] and choose a resolution of $128 \times 1024$ in the radial and horizontal direction, respectively. Grid refinement close to the top and bottom boundary is employed resulting in 10 km and 15 km thick cells at the surface and at the core-mantle boundary. To track composition, we use $4 \times 10^7$ tracers.

## 3. Results

### 3.1. Interaction of rifting and global dynamics

A typical example of rift evolution (Scenario A1) within our global convection model is shown in Fig.1, where a suture zone within collided continents is subjected to extension that finally leads to continental rupture and formation of a new ocean basin. Due to the self-consistent nature of our models, rifting events occur when the global buoyancy distribution generates a mantle configuration where the tensional force within the rift exceeds the strength of the suture between the two continents. This takes place when one or more of the following processes occur: (1) a subduction zone adjacent to the continent exerts an extensional force on the continent, (2) large-scale divergent mantle flow emerges beneath the suture dragging the continents away from each other, (3) a thermal plume impinges at the base of the suture, although this process is less important than the other two in our models. Regardless of the actual processes that contribute to the driving force of rifting, we find a characteristic rift evolution in all our scenarios that is described next.

Accepted Article

©2018 American Geophysical Union. All Rights Reserved.

In the pre-rift phase, prior to any divergence across the suture, the tensional stress within the continent progressively builds up until it reaches the yield limit within the suture (Fig.1k-m). Once this happens, divergence gradually starts with initially very slow rifting that continues over several tens of Myrs. At the same time the stress within the continent remains at maximum level. The accumulated extension across the rift gradually thins the thermal lithosphere leading to a decrease of rift strength, which in turn causes an increase in divergence velocity. The acceleration of rift velocity during the rift speed-up is mirrored by an abrupt stress drop (Fig.1n). Subsequently, the continents experience breakup at elevated velocity and a new ocean basin is formed. Inmodel A1, this happens by means of subduction initiation at a surprisingly large distance to the rift. After several tens of Myr of continental divergence, the global force balance eventually changes such that the continental stress increases again while the continents slow down and drift apart.

The evolution of model A1 is characteristic for many other model scenarios and can best be described by dividing it in several distinct phases (Fig.2). The pre-rift phase (phase 0) is accompanied by a gradual stress increase at zero extension velocity. Once tensional stresses reach the yield limit, initial rifting (phase 1) gradually starts at very low divergence velocities of less than 1 mm $yr^{-1}$ that slowly increase to about 10 mm $yr^{-1}$ within several tens of Myrs. During this phase, the stress load remains at maximum level before it suddenly drops by 80 % within ∼10 Myr. Simultaneously, rifting accelerates abruptly by more than one order of magnitude (phase 2) and remains at high divergence rates (phase 3) during the onset of sea-floor spreading. Within this stage, rift dynamics are governed by a positive feed-back loop between extension velocity and rift strength

©2018 American Geophysical Union. All Rights Reserved.

Accepted Article

loss, similar to a rope that is stretched until it yields and eventually snaps. Subsequently, the extension velocity drops to intermediate levels of several tens of mm $yr^{-1}$ while the continental stress increases again (phase 4).

The characteristic history of extension velocity and continental stress is robustly reproduced by alternative scenarios (Supplementary Table 1). We analyze three groups of models (A, B and C) differing in lithospheric strengththat controls the number and size of the plates (models A and B have strong oceanic lithosphere and larger plates compared to the model group C with weak oceanic lithosphere and smaller plates). Secondly, the models differ in the strength limit within the continents (high yield strength for models A and no yield limitation for models B and C) that has only minor influence on the dynamics of the system. Cases within one model group (e.g. A1, A2, etc.) represent different rift events for a model with the same parameters but different initial conditions, i.e. other random snapshots from the equilibrated part of the evolution. All ten scenarios depicted in Fig.2c feature the slow initial rift stage followed by abrupt rift acceleration and a high extension rate during the onset of sea-floor spreading. The shape of individual velocity histories is very similar during phase 1 and 2, however, it differs during phases 3 and 4. During the post-rift phase, 7 out of 10 examples exhibit a distinct decrease of post-breakup divergence velocity similar to scenario A1, whereas two examples remain at maximum velocities for more than 40 Myr (B1, C2), while in another scenario the extension velocity increases even further (A2). The reason for this diversity lies again in the different mantle and plate boundary configurations that exert the dominant control on the kinematic evolution during the post-rift phase.

©2018 American Geophysical Union. All Rights Reserved.

Accepted Article

### 3.2. Comparison with tectonic reconstructions

Reconstructions of Pangea breakup not only illustrate the velocity increase during rifting [Brune et al., 2016] suggested by observations from passive margins, but theyalso provide quantitative constraints on the evolution of relative plate velocities after breakup through linear magnetic anomalies associated with crust formed by sea-floor spreading. Figure 3 shows the plate kinematic history for 6 successful rifts discussed by Brune et al. [2016], which evolved into sustained sea-floor spreading with spreading rate variations recorded across >20 Myr. Decreases in divergence rate within 30 Myr after the speed-up are recorded in the North Atlantic, Central Atlantic, and Australia-Antarctic basins, whereas the divergence rate continues to slowly increase between North America and Greenland. Both the South Atlantic and Iberia-North America rifts reach breakup around the beginning of the Cretaceous Normal Superchron (CNS), a period of >35 Myr during which no isochrons due to magnetic polarity reversals are available to quantitatively constrain changes in divergence rates. Analysis of magnetic anomalies due to variations in magnetic field strength during the CNS [Granot and Dyment, 2015] suggest a progressive increase in divergence rates from ∼120 Ma until ∼80 Ma before dropping in the latest Cretaceous.

Several caveats need to be kept in mind when comparing natural examples to our model results. Changes in divergence rates for these natural examples may be explained by factors not included in the geodynamic models - for example, the collision of Greenland with Ellesmere Island shortly after breakup between Greenland and Eurasia may explain the pronounced slowdown in North Atlantic divergence rates [Gaina et al., 2009]. The rela-

©2018 American Geophysical Union. All Rights Reserved.

Accepted Article

tionship between the timing of rift velocity increase and breakup is likely to differ between our 2D models and natural examples (where breakup is defined by the onset of seafloor spreading). This is due to the fact that(1) progressive unzipping of continents on a spherical Earth persisting for 25 Myr (e.g. South Atlantic) or more (e.g. Australia-Antarctica), means that breakup for natural examples is prolonged and complex compared to the relatively discrete breakup in the 2D models, and (2) in nature, continental extension or mantle exhumation may continue for significant periods beyond the time of rift-strength loss resulting in a delay between rift velocity increase and breakup (Fig.3), whereas this process is not captured in our 2D model cases (and we instead define breakup for the model cases as the moment of lithospheric rupture). The timing of velocity changes in Figure 3 is dependent on the timing of interpreted magnetic isochrons, and the relatively coarse sampling of these isochrons in many basins (∼5–10 Myr, and much greater in the CNS) allows for greater variability in initial spreading rates than captured by reconstructions [Lundin et al., 2018].

## 4. Discussion and conclusion

It has been previously suggested that continental rifting typically involves a slow-fast kinematic evolution due to the interaction of internal rift weakening with far-field plate driving forces [Brune et al., 2016]. Here we reproduce the previous findings concerning the rift stage, but also gain new insight concerning the post-rift evolution. Phase 1 corresponds to the initial rift stage of slow rifting where the extensional stress level is controlled by the lithospheric yield strength. Phase 2 comprises the rift acceleration period and is marked by an abrupt increase of extension rate and a simultaneous stress

©2018 American Geophysical Union. All Rights Reserved.

Accepted Article

drop that corresponds to rift strength loss due to necking of the lithosphere. Note that the coeval change in velocity and stress can only be addressed in models without lateral boundaries, i.e without prescribing either a boundary velocity or a boundary force. The fact that we reproduce previously suggested rift kinematics with a more general model setup therefore lends further robustness to these findings. Continental breakup takes place at the beginning of phase 3, and hence, extension velocity during phase 3 is no longer controlled by rift strength but by the global force balance. The different amplitudes of the presented models therefore relate to the diverse mantle and plate boundary configurations in the individual models. Maximum post-rift velocities last from 5 My to more than 40 My depending on the longevity of mantle structure and plate boundary configuration. Many models display a distinct phase 4 where divergence velocities decrease gradually. This can be understood when considering that only certain combinations of mantle drag and plume impingement beneath the continent or subduction geometries adjacent to the continent generate sufficient tensional stress to overcome the lithospheric strength at the continental suture. During the post-rift phase, these configurations typically continue driving the plates in the same directions at an elevated speed, however, the velocity of the plates is prone to decrease once the large-scale configuration eventually changes.

Since the surface area of the Earth is constant, every change in rift kinematics has to be compensated by changes in relative motion at other plate boundaries. The abrupt velocity increase during phase 2 therefore induces enhanced convergence in many model scenarios. This model outcome predicts enhanced subduction velocities, for instance for North America and the Farallon plate during Central Atlantic rifting in the Early Jurassic,

Accepted Article

©2018 American Geophysical Union. All Rights Reserved.

or closure of back-arc basins as inferred in the proto-Andean ranges of South America during South Atlantic opening [Maloney et al., 2013]. Interestingly, compensation of rift acceleration does not necessarily take place adjacent to the two plates involved in the rift event, but often occurs in locations far from the model continents. Scenarios A1, B1, and C1, for instance, exhibit subduction initiation at large distance from the continents, contemporaneous to the rift acceleration (see supplementary animations). A similar effect takes place in scenario A2, where the convergence rate at distant subduction zones rapidly increases during rift phase 3. To quantify the link between rifting and subduction initiation in a statistical way, we analyzed the strong lithosphere scenarios (model groups A and B) where the number of subduction zones is best representative of Earth. Of these 8 rift scenarios, 5 events feature subduction initiation within 15 My before breakup. Additionally, these models exhibit subduction initiation on average $\sim$2.4 times per 100 My, independent of rift occurrence. Hence, the probability for subduction initiation during 15 My is 0.63 during a rift event, but almost two times lower, namely 0.36, without rifting. Due to the low number of rift cases the rift-related probability includes a degree of uncertainty, nevertheless the impact of rifting on subduction initiation appears to be statistically significant. We speculate that existing subduction zones do not actually constitute weak spots thateasily accommodate more convergence. Instead, the cold and rigid subducting slabs (see Fig. 1) connect the high-viscosity lithosphere to the high-viscosity lower mantle. Due to this coupling, rift-related displacements of the lithosphere cannot always change the convergence rate at an existing subduction zone and instead may induce subduction initiation at another location. However, subduction inception

©2018 American Geophysical Union. All Rights Reserved.

Accepted Article

very far from the continents might be biased due to the 2D character of our simulations. In 3D geometry, there may be more ways to accommodate the increased divergence as mantle flow and plate motions can occur in orthogonal direction to the 2D plane and hence change the location of subduction initiation.

These results point to a causal relationship between rift acceleration and global plate reorganization. Global plate tectonic reconstructions reveal abrupt, widespread changes in plate motion and boundary configurations, notably at ∼50 and ∼100 My ago [Whittaker et al., 2007; Matthews et al., 2012], which have variably been attributed to ridge subduction, plume-push forces, and continent-continent collision. Eocene plate motion change is contemporaneous with the initiation of major new intra-oceanic subduction zones across a wide region of the western Pacific presently represented by the Izu-Bonin-Mariana and Tonga-Kermadec systems [Gurnis et al., 2004]. Current hypotheses suggest a role for both local lithospheric buoyancy variations and plate-scale compressional forces [Arculus et al., 2015; Sutherland et al., 2017], yet the ultimate trigger for these new plate boundaries to form by either mechanism remains unclear. Our model results allow us to propose the far-field effect of rift acceleration and breakup in the North Atlantic and Eurasia Basin (∼55 My ago) as an alternative, plausible catalyst for distal, almost contemporaneous changes in plate boundary configuration and force balance. The details of earlier subduction initiations are less clear, but mid-Cretaceous subduction initiation within the Tethys ocean [Maffione et al., 2017; Guilmette et al., 2018] could be connected to increases in rift velocity within the South Atlantic and between Australia and Antarctica.

Accepted Article

©2018 American Geophysical Union. All Rights Reserved.

When interpreting the numerical results one should keep in mind that there are certain model limitations. Several lithospheric weakening mechanisms are not accounted for such as strain softening, intrusion-related heating, shear heating, and structural softening [Huismans et al., 2005; Duretz et al., 2015, 2016]. Lithospheric deformation of plate boundaries on Earth has a memory of previous yielding, but our rheological description neglects any deformation history and reflects instantaneous stress distribution. Therefore, the change in extension rate in our convection models must be seen as a lower bound to the rift acceleration in nature. In the model design, we made a number of assumptions that might influence the style of rifting. Importantly, we fix the internal heating rate so that plumes in the models are weak and do not add much driving force for rifting. Decreasing the internal heating and thus increasing the strength of the plumes might result in plume-induced rifting [Koptev et al., 2015]. Also, rifting might be facilitated by having weak continental margins [Rolf et al., 2014] while here we assume them to have the same rigidity as the continental interior. Timing of rifting is related to the mantle structures such as size of convective cells [Rolf et al., 2014] that are probably larger here compared to the Earth due to the lower convective vigour, which lead us to employ a transit time framework to scale the results and compare them to observations. Employing standard scaling using the diffusive time would result in $\sim$4 times lower rift velocities, while simultaneously leading to $\sim$4 times longer durations of each rift phase. Ideally, both scalings should result in the same average Earth-like velocities, given that we use "realistic" Earth parameters representing our planet including a suitable rheological law. Note that using a

©2018 American Geophysical Union. All Rights Reserved.

Accepted Article

different scaling formulation would affect the absolute values in Fig.2, but does not change our overall conclusions.

A major advantage of the presented models over previous Cartesian box rift models with velocity or force boundary conditions is that the spherical annulus geometry does not require lateral boundary conditions to be specified, simply because there are no lateral boundaries. While it is not computationally feasible for mantle convection models to employ high resolution and complex rheology as is commonly employed in lithospheric-scale setups, the new results can nevertheless be used to infer which type of boundary condition in Cartesian box simulations is most realistic for a given setting. (1) If the modeling setup focuses on lithospheric-scale weakening processes and the associated stress evolution during phase 1, we find that constant force boundary conditions are most appropriate, because the stress during this phase is almost constant (Fig.2b). (2) If however the setup addresses late rift stages or the transition from rifting to sea-floor spreading, we recommend constant velocity boundary conditions, since the divergence velocity does not change much during phase 3. The same is true when investigating the evolution of a small basin where there is no feedback between rift dynamics and large scale plate motions. Note that during phase 2, the global force balance interacts with the rift-strength loss and neither local nor global processes can be neglected.

In summary, we conclude that geodynamic and plate tectonic modeling suggests a multi-phase velocity behavior during continental rifting that is controlled by the interaction of rift dynamics with far-field forces. In our models, rifting involves a characteristic speed-up and often a later slow down of plate divergence, comparable with natural examples.

Accepted Article

©2018 American Geophysical Union. All Rights Reserved.

These changes in plate motion are expected to be mirrored elsewhere either by enhanced convergence rates at an existing trench or through initiation of a new subduction zone.

**Acknowledgments.** The support for this research has been provided by the European Union's Horizon 2020 research and innovation program under the ERC grant agreement n°617588 and the Marie Skłodowska Curie grant agreement n°753755, the German Academic Exchange Service (DAAD) project n°57319603, the Helmholtz Association through the Young Investigators Group CRYSTALS (n°VH-NG-1132), and Australian Research Council grants n°IH130200012 and n°DP180102280. Simulations were performed on the AUGURY super-computer at P2CHPD Lyon. The StagPy library was used in this study to process StagYY output data (`https://github.com/StagPython/StagPy`). The authors thank N. Coltice for his comments on this work, P. Tackley for providing the StagYY code, and T. Rolf and S. Buiter for constructive and motivating reviews that helped to improve the manuscript. Data used to run the StagYY are available in the supplementary material.

## References

Ammann, N., Liao, J., Gerya, T., Ball, P., 2017. Oblique continental rifting and long transform fault formation based on 3d thermomechanical numerical modeling. Tectonophysics doi:10.1016/j.tecto.2017.08.015.

Arculus, R.J., Ishizuka, O., Bogus, K.A., Gurnis, M., Hickey-Vargas, R., Aljahdali, M.H., Bandini-Maeder, A.N., Barth, A.P., Brandl, P.A., Drab, L., et al., 2015. A record of spontaneous subduction initiation in the Izu-Bonin-Mariana arc. Nat. Geosci. 8,

©2018 American Geophysical Union. All Rights Reserved.

Accepted Article

728–733.

Armitage, J.J., Petersen, K.D., Pérez-Gussinyé, M., 2018. The role of crustal strength in controlling magmatism and melt chemistry during rifting and breakup. Geochem., Geophys., Geosyst. 19, 534–550.

Brune, S., 2016. Rifts and rifted margins: A review of geodynamic processes and natural hazards. Plate Boundaries and Natural Hazards 219, 11–37.

Brune, S., 2018. Forces within continental and oceanic rifts: Numerical modeling elucidates the impact of asthenospheric flow on surface stress. Geology 46, 191.

Brune, S., Heine, C., Clift, P.D., Pérez-Gussinyé, M., 2017. Rifted margin architecture and crustal rheology: reviewing Iberia-Newfoundland, central South Atlantic, and South China sea. Marine and Petroleum Geology 79, 257–281.

Brune, S., Heine, C., Pérez-Gussinyé, M., Sobolev, S.V., 2014. Rift migration explains continental margin asymmetry and crustal hyper-extension. Nature Communications 5, 4014.

Brune, S., Popov, A.A., Sobolev, S.V., 2012. Modeling suggests that oblique extension facilitates rifting and continental break-up. Journal of Geophysical Research: Solid Earth 117.

Brune, S., Popov, A.A., Sobolev, S.V., 2013. Quantifying the thermo-mechanical impact of plume arrival on continental break-up. Tectonophysics 604, 51–59.

Brune, S., Williams, S.E., Butterworth, N.P., Müller, R.D., 2016. Abrupt plate accelerations shape rifted continental margins. Nature 536, 201–204.

©2018 American Geophysical Union. All Rights Reserved.

Accepted Article

Buck, W., 2015. Dynamic processes in extensional and compressional settings: The dynamics of continental breakup and extension, in: Schubert, G. (Ed.), Treatise on Geophysics. Elsevier, Oxford, Second edition. pp. 325–379.

Coltice, N., Gérault, M., Ulvrová, M., 2017. A mantle convection perspective on global tectonics. Earth-Sci. Rev. 165, 120 – 150.

Coltice, N., Rolf, T., Tackley, P.J., Labrosse, S., 2012. Dynamic causes of the relation between area and age of the ocean floor. Science 336, 335–338.

Crameri, F., Tackley, P.J., Meilick, I., Gerya, T.V., Kaus, B.J.P., 2012. A free plate surface and weak oceanic crust produce single-sided subduction on earth. Geophys. Res. Lett. 39. L03306.

Davis, J.K., Lavier, L.L., 2017. Influences on the development of volcanic and magma-poor morphologies during passive continental rifting. Geosphere 13, 1524–1540.

Doin, M.P., Fleitout, L., Christensen, U., 1997. Mantle convection and stability of depleted and undepleted continental lithosphere. J. Geophys. Res.: Solid Earth 102, 2771–2787.

Duretz, T., Petri, B., Mohn, G., Schmalholz, S.M., Schenker, F.L., Mntener, O., 2016. The importance of structural softening for the evolution and architecture of passive margins. Scientific Reports 6, 38704.

Duretz, T., Schmalholz, S.M., Podladchikov, Y.Y., 2015. Shear heating-induced strain localization across the scales. Philosophical Magazine 0, 1–16.

Forsyth, D., Uyeda, S., 1975. On the relative importance of the driving forces of plate motion. Geophys. J. R. Astr. Soc. 43, 163–200.

©2018 American Geophysical Union. All Rights Reserved.

Accepted Article

Gaina, C., Gernigon, L., Ball, P., 2009. Palaeocene–recent plate boundaries in the NE Atlantic and the formation of the Jan Mayen microcontinent. Journal of the Geological Society 166, 601–616.

Gerya, T.V., Connolly, J.A., Yuen, D.A., 2008. Why is terrestrial subduction one-sided? Geology 36, 43–46.

Granot, R., Dyment, J., 2015. The Cretaceous opening of the South Atlantic Ocean. Earth Planet. Sci. Lett. 414, 156–163.

Guilmette, C., Smit, M.A., van Hinsbergen, D.J.J., Grer, D., Corfu, F., Charette, B., Maffione, M., Rabeau, O., Savard, D., 2018. Forced subduction initiation recorded in the sole and crust of the Semail ophiolite of Oman. Nat. Geosci. 11, 688–695.

Gurnis, M., Hall, C., Lavier, L., 2004. Evolving force balance during incipient subduction. Geochem., Geophys., Geosyst. 5. Q07001.

Heine, C., Brune, S., 2014. Oblique rifting of the Equatorial Atlantic: why there is no Saharan Atlantic Ocean. Geology 42, 211–214.

Heine, C., Zoethout, J., Müller, R., 2013. Kinematics of the South Atlantic rift. Solid Earth 4, 215–253.

Hernlund, J.W., Tackley, P.J., 2008. Modeling mantle convection in the spherical annulus. Phys. Earth Planet. Inter. 171, 48–54.

Huismans, R.S., Beaumont, C., 2003. Symmetric and asymmetric lithospheric extension: Relative effects of frictional-plastic and viscous strain softening. J. Geophys. Res.: Solid Earth 108. 2496.

Accepted Article

©2018 American Geophysical Union. All Rights Reserved.

Huismans, R.S., Buiter, S.J.H., Beaumont, C., 2005. Effect of plastic-viscous layering and strain softening on mode selection during lithospheric extension. Journal of Geophysical Research-Solid Earth 110, –.

Jaupart, C., Labrosse, S., Lucazeau, F., Mareschal, J., 2015. 7.06 - temperatures, heat and energy in the mantle of the earth, in: Schubert, G. (Ed.), Treatise on Geophysics (Second Edition). Elsevier, Oxford. volume 7, Second edition edition. pp. 223–270.

Kneller, E.A., Johnson, C.A., Karner, G.D., Einhorn, J., Queffelec, T.A., 2012. Inverse methods for modeling non-rigid plate kinematics: Application to mesozoic plate reconstructions of the Central Atlantic. Computers & Geosciences 49, 217–230.

Koptev, A., Calais, E., Burov, E., Leroy, S., Gerya, T., 2015. Dual continental rift systems generated by plume–lithosphere interaction. Nat. Geosci. 8, 388–392.

Lenardic, A., Moresi, L.N., 1999. Some thoughts on the stability of cratonic lithosphere: Effects of buoyancy and viscosity. J. Geophys. Res.: Solid Earth 104, 12747–12758.

Lundin, E.R., Doré, A.G., Redfield, T.F., 2018. Magmatism and extension rates at rifted margins. Petroleum Geoscience doi:10.1144/petgeo2016-158.

Maffione, M., van Hinsbergen, D.J., de Gelder, G.I., van der Goes, F.C., Morris, A., 2017. Kinematics of Late Cretaceous subduction initiation in the Neo-Tethys Ocean reconstructed from ophiolites of Turkey, Cyprus, and Syria. J. Geophys. Res.: Solid Earth 122, 3953–3976.

Maloney, K.T., Clarke, G.L., Klepeis, K.A., Quevedo, L., 2013. The Late Jurassic to present evolution of the Andean margin: Drivers and the geological record. Tectonics 32, 1049–1065.

©2018 American Geophysical Union. All Rights Reserved.

Accepted Article

Matthews, K.J., Seton, M., Müller, R.D., 2012. A global-scale plate reorganization event at 105–100 Ma. Earth Planet. Sci. Lett. 355-356, 283 – 298.

McQuarrie, N., Wernicke, B.P., 2005. An animated tectonic reconstruction of southwestern North America since 36 Ma. Geosphere 1, 147–172.

Mondy, L.S., Rey, P.F., Duclaux, G., Moresi, L., 2017. The role of asthenospheric flow during rift propagation and breakup. Geology 46, 103–106.

Moresi, L., Solomatov, V., 1998. Mantle convection with a brittle lithosphere: thoughts on the global tectonic styles of the earth and venus. Geophys. J. Int. 133, 669–682.

Müller, R.D., Seton, M., Zahirovic, S., Williams, S.E., Matthews, K.J., Wright, N.M., Shephard, G.E., Maloney, K.T., Barnett-Moore, N., Hosseinpour, M., Bower, D.J., Cannon, J., 2016. Ocean Basin Evolution and Global-Scale Plate Reorganization Events Since Pangea Breakup. Ann. Rev. Earth Planet. Sci. 44, 107–138.

Naliboff, J., Buiter, S.J.H., 2015. Rift reactivation and migration during multiphase extension. Earth Planet. Sci. Lett. 421, 58–67.

Pérez-Gussinyé, M., Morgan, J.P., Reston, T.J., Ranero, C.R., 2006. The rift to drift transition at non-volcanic margins: Insights from numerical modelling. Earth Planet. Sci. Lett. 244, 458–473.

Rolf, T., Capitanio, F., Tackley, P., 2017. Constraints on mantle viscosity structure from continental drift histories in spherical mantle convection models. Tectonophysics doi:10.1016/j.tecto.2017.04.031.

Rolf, T., Coltice, N., Tackley, P., 2014. Statistical cyclicity of the supercontinent cycle. Geophys. Res. Lett. 41, 2351–2358.

©2018 American Geophysical Union. All Rights Reserved.

Accepted Article

Rolf, T., Tackley, P., 2011. Focussing of stress by continents in 3D spherical mantle convection with self-consistent plate tectonics. Geophys. Res. Lett. 38. L18301.

Salerno, V.M., Capitanio, F.A., Farrington, R.J., Riel, N., 2016. The role of long-term rifting history on modes of continental lithosphere extension. J. Geophys. Res.: Solid Earth 121, 8917–8940.

Seton, M., Mller, R., Zahirovic, S., Gaina, C., Torsvik, T., Shephard, G., Talsma, A., Gurnis, M., Turner, M., Maus, S., Chandler, M., 2012. Global continental and ocean basin reconstructions since 200 Ma. Earth-Science Reviews 113, 212–270.

Sutherland, R., Collot, J., Bache, F., Henrys, S., Barker, D., Browne, G., Lawrence, M., Morgans, H., Hollis, C., Clowes, C., et al., 2017. Widespread compression associated with Eocene Tonga-Kermadec subduction initiation. Geology 45, 355–358.

Tackley, P.J., 2000a. The Quest for Self-Consistent Generation of Plate Tectonics in Mantle Convection Models. American Geophysical Union, Washington, D.C.. volume 121 of *Geophys. Monograph.* pp. 47–72.

Tackley, P.J., 2000b. Self-consistent generation of tectonic plates in time-dependent, three-dimensional mantle convection simulations 1. pseudoplastic yielding. Geochem., Geophys., Geosyst. 1. 2000GC000036.

Tackley, P.J., 2008. Modelling compressible mantle convection with large viscosity contrasts in a three-dimensional spherical shell using the yin-yang grid. Phys. Earth Planet. Inter. 171, 7–18.

Tackley, P.J., King, S.D., 2003. Testing the tracer ratio method for modeling active compositional fields in mantle convection simulations. Geochem., Geophys., Geosyst.

©2018 American Geophysical Union. All Rights Reserved.

Accepted Article

4, 8302.

Tagawa, M., Nakakuki, T., Kameyama, M., Tajima, F., 2007. The role of history-dependent rheology in plate boundary lubrication for generating one-sided subduction. Pure Appl. Geophys. 164, 879–907.

Takeshita, T., Yamaji, A., 1990. Acceleration of continental rifting due to a thermomechanical instability. Tectonophysics 181, 307–320.

Tetreault, J., Buiter, S., 2018. The influence of extension rate and crustal rheology on the evolution of passive margins from rifting to break-up. Tectonophysics 746, 155 – 172. Understanding geological processes through modelling - A Memorial Volume honouring Evgenii Burov.

Turcotte, D.L., Schubert, G., 2002. Geodynamics. Cambridge University Press. 2 edition.

Whittaker, J.M., Müller, R.D., Leitchenkov, G., Stagg, H., Sdrolias, M., Gaina, C., Goncharov, A., 2007. Major Australian-Antarctic plate reorganization at Hawaiian-Emperor Bend time. Science 318, 83–86.

Ziegler, P.A., Cloetingh, S., 2004. Dynamic processes controlling evolution of rifted basins. Earth-Science Reviews 64, 1–50.

Accepted Article

©2018 American Geophysical Union. All Rights Reserved.

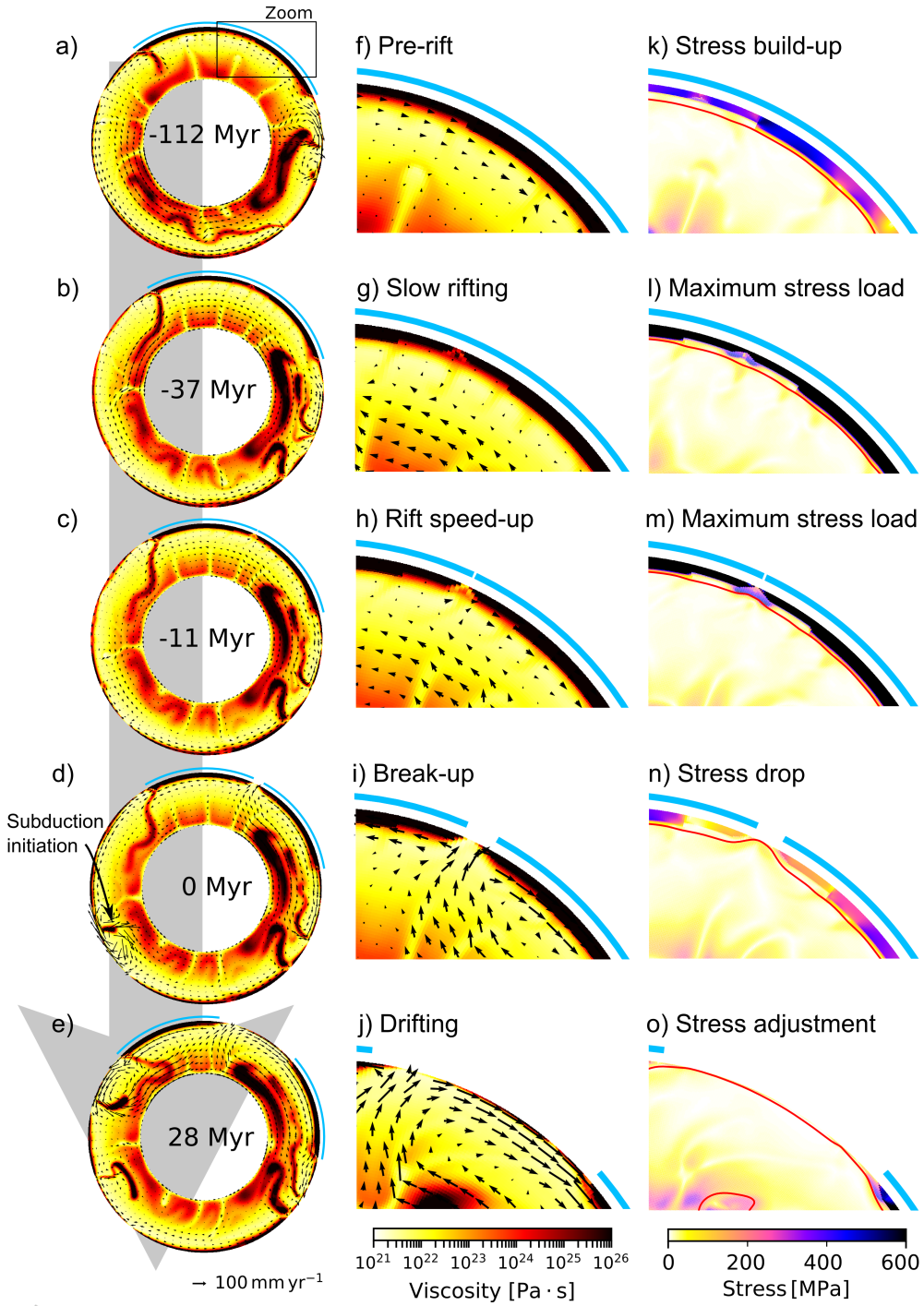


**Figure 1.** Evolution of reference model A1. (a-e) Mantle viscosity is depicted with velocity arrows in the left column. Time is increasing downwards and breakup occurs at 0 Myr. (f-o) Close-up viscosity together with the second invariant of the stress tensor are shown in the middle and right column, respectively. The 1200 °C isotherm is shown by red line in the right column. Zoom area is depicted in (a). For visual reference the position of the continents is emphasized in blue. Corresponding rift velocity and stress time series are depicted in Fig. 2a,b. The full model animation can be found in the supplementary materials.

©2018 American Geophysical Union. All Rights Reserved.

Accepted Article

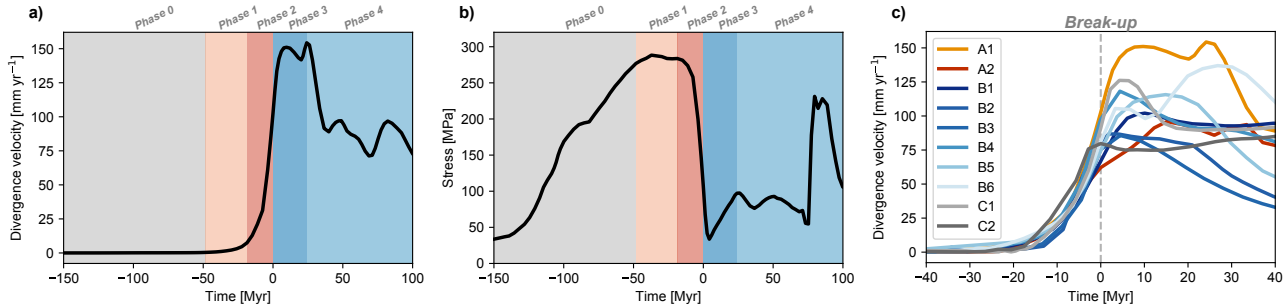


**Figure 2.** Temporal evolution of divergence velocity and stress. (a) Relative velocity of the continents in model scenario A1 (see Fig. 1 for spatio-temporal evolution). (b) Second invariant of the stress tensor in the cratonic continental areas of scenario A1. An average of the stress in the center of the two future continents just below the surface at depth around 10 km is displayed. (c) Rift velocity for all simulated rift cases. Breakup is marked by the dashed vertical line. In all panels, 0 Myr corresponds to breakup time. See supplementary materials for animations of selected scenarios A1, A2, B1, and C1.

©2018 American Geophysical Union. All Rights Reserved.

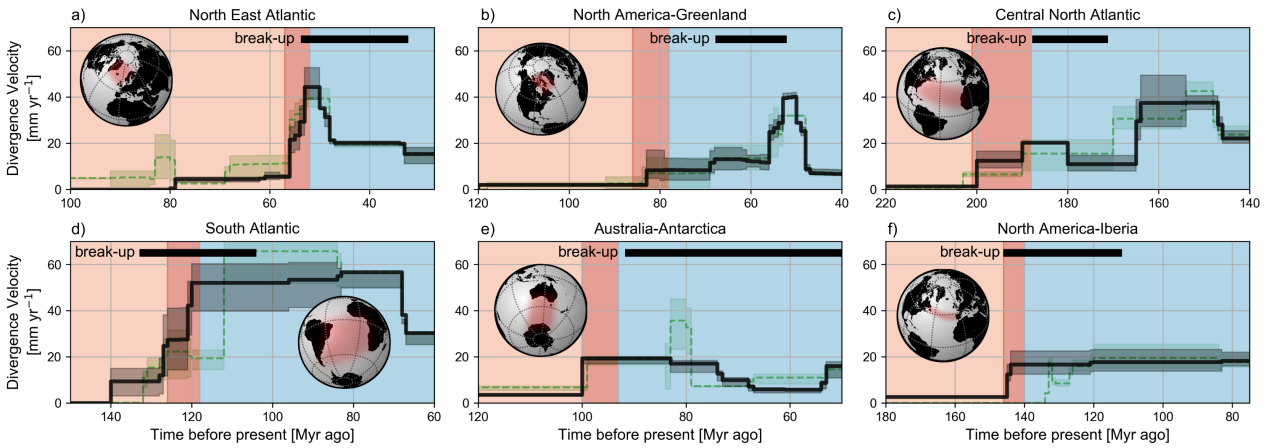


**Figure 3.** Continent divergence rates from plate tectonic reconstructions. Black curves illustrate velocity evolution for seed points within the central segment of each rift using reconstruction parameters described in Brune et al. [2016], with bounding grey regions illustrating the variability of rift velocity across the full extent of the rift system. Light green curves show equivalent results using the alternative reconstructions collated by Seton et al. [2012]. The black bar at the top of each panel defines the timespan of diachronous breakup [see Brune et al., 2016, for detail].

©2018 American Geophysical Union. All Rights Reserved.

Accepted Article